Available online at www.sciencedirect.com

ScienceDirect

IFAC Papers Online CONFERENCE PAPER ARCHIVE

IFAC PapersOnLine 50-1 (2017) 14626–14631

Refining Dynamics Identification for Co-Bots: Case Study on KUKA LWR4+ ⋆

Sergey A. Kolyubin * **Anton S. Shiriaev** ** **Anthony Jubien** ***

* *Dept. of Computer Science and Control Systems, ITMO University, 197101 St. Petersburg, Russia (e-mail: s.kolyubin@corp.ifmo.ru).*
** *Dept. of Engineering Cybernetics, NTNU, NO-7491 Trondheim, Norway (e-mail: anton.shiriaev@ntnu.no)*
*** *Nantes Digital Sciences Laboratory LS2N, 44300 Nantes, France (email: anthony.jubien@univ-nantes.fr)*

Abstract: This paper presents an attempt to improve dynamic identification procedure for robotic manipulators, such that obtained models are appropriate for trajectory planning and motion control. In addition to algorithms development, authors bring new insights and arguments for the experiments organisation and analysis of the collected data. Significant part of the work is devoted to a case study in calibrating of a collaborative robot (co-bot) KUKA LWR4+, which represents a powerful tool for modern manufacturing systems. Therefore, refined models compared to the ones relied on CAD data provided by the manufacturer can be beneficial for various applications.

Keywords: Model identification, robotic manipulators, model-based control, motion planning.

1. INTRODUCTION

Developing an accurate dynamic model for robotic manipulators is necessary for either its rigorous simulation and trajectories planning or high-performance control. Erroneous estimates of robot parameters used by a motion planner or a controller can significantly degrade the overall system performance.

Being appropriate for some assignments, CAD models provided by a manufacturer require refinements for others tasks, where neglected or averaged effects due to motors' dynamics, friction, non-uniform mass distribution of links and robot-to-robot variations should be taken into account.

This challenge has stimulated quite many works to appear for the last several years. For example, only the problem of KUKA light-weight arm dynamics calibration were consider in Bargsten et al. (2013); Briot et al. (2014); Gaz et al. (2014); Jubien et al. (2014a,b); Rackl et al. (2012). Rackl et al. (2012) and Bargsten et al. (2013) are one of the early results on KUKA LWR4+ parameters identification, but both works are using a simplified model that neglects motor dynamics. Rackl et al. (2012) proposes an approach of planning excitation trajectories parametrised as B-splines, therefore it requires a post-analysis to avoid critical frequencies excitation. Bargsten et al. (2013) lacks experimental data pre-processing step and confidence evaluation for the obtained estimates. Gaz et al. (2014) considers the same task to be solved by the reverse engineering approach, when estimates are based not on the position and torque measurements collected along continuous trajectories, but on the data provided by the robot software at static positions only. It also differs in terms of the parametric dynamics representation, where the coupling of the robot and motor dynamics were described through the deflection model and Hooke's law. This study is based on the procedures described in Briot et al. (2014); Jubien et al. (2014a,b). However, in these works excitation works are restricted to be point-to-point movements with trapezoidal acceleration profiles.

Here we focus on the off-line estimation of the robot dynamic parameters. State-of-the-art techniques were applied and experimentally verified here. We enhanced the approach from Briot et al. (2014); Jubien et al. (2014a,b) with the novel calibration trajectories optimisation algorithm that provides better excitation and consequently improves estimation accuracy. Recommendations on calibration trajectories initial parameters, active constraints, algorithms tuning, and experimental data filtering are provided throughout the paper.

The significant part of the discussed identification procedure has been implemented on the KUKA Light-Weight Robot (LWR4+), which is a redundant serial manipulator with 7 rotational joints and serves as one of popular and widely used platforms in robotics research specifically for developing and testing new motion planning, HMI, and motion control algorithms.

Experimental study in this work was done with KUKA LWR4+ different from the one tested in Jubien et al. (2014b), which gives a basis for comparative analysis of the robot-to-robot parameters variation.

The rest of the paper is organised in the following way. We start from a problem statement. Then, a model suitable for identification purposes is derived. After, we introduce an approach for optimising identification trajectories and

⋆ This work was supported by the Government of the Russian Federation, GOSZADANIE no. 8.8885.2017/BP and Grant 074-U01.

10.1016/j.ifacol.2017.08.1741

continue with parameters estimation algorithms. Finally, we describe an experimental setup and discuss case-study results.

2. DYNAMIC MODEL

The dynamics of an open-chain manipulator with n-degrees of freedom and physically collocated actuators having substantial gear-ratios in transmission [1] can be well approximated by the *Inverse Dynamics Model (IDM)*

$$\tau_l = M(q)\ddot{q} + C(q,\dot{q})\dot{q} + G(q) + \tau_{fl}, \quad (1)$$

$$\tau = I_a\ddot{q} + \tau_l + \tau_{fm}. \quad (2)$$

Here q, $\dot{q}$, and $\ddot{q} \in \mathbb{R}^n$ are vectors of joint positions, velocities, and accelerations; τ and $\tau_l \in \mathbb{R}^n$ are vectors of motor and joint torques; $M(q)$ is $n \times n$ link inertia matrix; $C(q,\dot{q})\dot{q}$ and $G(q) \in \mathbb{R}^n$ are vectors representing Coriolis/centrifugal generalised forces and forces due to gravity or compliance; I_a is the diagonal drive inertia matrix (motor and gearbox); τ_{fm} and $\tau_{fl} \in \mathbb{R}^n$ are vectors of motor and joint friction torques. Eq. (2) can be obtained via Newton-Euler or Lagrangian approaches Khalil and Dombre (2004).

The identification task requires also a parametrization of dissipative generalized forces represented in Eqns. (1)-(2) in the lump format as torques τ_{fl} and τ_{fm}. The simplest parametric model of a friction includes symmetric and decoupled Coulomb and linear viscous parts solely dependent on links' angular velocities

$$\tau_{fl} = F_{vl}\dot{q} + F_{cl}\mathtt{sign}(\dot{q}) + offl, \quad (3)$$

$$\tau_{fm} = F_{vm}\dot{q} + F_{cm}\mathtt{sign}(\dot{q}) + offm. \quad (4)$$

Here F_{vm}, F_{cm}, F_{vl} and F_{cl} are $n \times n$ diagonal constant matrices of viscous and Coulomb friction coefficients for motors and joints respectively; $offm$ and $offl \in \mathbb{R}^n$ are motor and joint torque offsets.

As known (see e.g. Hollerbach et al. (2008); Gautier and Khalil (1990); Khalil and Dombre (2004)), the nonlinear Eqns. (1)-(4) of the robot dynamics are linear in so called *barycentric parameters*

$$\tau(t) = \omega\left(q(t),\dot{q}(t),\ddot{q}(t)\right)\chi, \quad \forall t. \quad (5)$$

The $[n \times n_s]$ matrix function $\omega(\cdot)$ represents the *IDM Jacobian* with respect to a vector of parameters $\chi = [\chi_1;\ldots;\chi_n] \in \mathbb{R}^{n_s}$, where

$$\chi_j = [XX_j, XY_j, XZ_j, YY_j, YZ_j, ZZ_j, MX_j, MY_j, MZ_j, M_j, I_{aj}, F_{vl,j}, F_{cl,j}, offl_j, F_{vm,j}, F_{cm,j}, offm_j]^T$$

with XX_j, XY_j, XZ_j, YY_j, YZ_j, and ZZ_j being the inertia tensors, MX_j, MY_j, and MZ_j being the first moments, M_j being the mass all listed for the j-th link, $j = 1,\ldots,n$; and with $n_s = 17 \cdot n$ being the total number of barycentric parameters.

Remark 1. An efficient way of calculating the IDM in a form (5) is to use spatial vector notation and Recursive Newton-Euler Algorithm (RNEA) or its modifications Featherstone and Orin (2008).

[1] According to DLR Light-Weight Robot III specifications `http://www.dlr.de/rmc/rm/en/desktopdefault.aspx/tabid-3803/6175_read-8963/` (the predecessor of the KUKA LWR4+) all seven harmonic drives have high gear ratios. In particular, they are 1:100 for axes 1, 2, 3, 4, 6, and 7; and 1:160 for axis 5.

The representation (5) is often redundant and some of parameters might not be identifiable. Therefore, one searches for a subset of n_b *base IDM parameters* χ_B with $n_b \leq n_s$, which are sufficient for reconstructing the motors' torques in the left-hand-side of Eqn. (5)

$$\tau(t) = \omega_B\left(q(t),\dot{q}(t),\ddot{q}(t)\right)\chi_B, \quad \forall t. \quad (6)$$

Here $\omega_B(\cdot)$ known as the *base IDM Jacobian* $[n \times n_b]$ matrix is composed from n_b columns of $\omega(\cdot)$ originally defined by the dynamics in (5).

Remark 2. Sets of base parameters can be determined using closed-form rules of Khalil et al. (1991) or QR-decomposition of the IDM Jacobian (see e.g. Khalil and Gautier (1991)).

Motivated by practical use, we assume that the following model reproduces the measurements accurately

$$\tau_m(t) = \omega_B\left(q_m(t),\dot{q}_m(t),\ddot{q}_m(t)\right)\chi_B + \epsilon(t), \quad (7)$$

i.e. the noise $\epsilon(t)$ that appears in measurements $q_m(\cdot)$, $\tau_m(\cdot)$ and enters into coefficients of the regressor $\omega_B(\cdot)$ is additive.

After, we collect measurements, while the robot is moving along a certain trajectory, and augment the data into the overdetermined set of linear equations

$$\Upsilon = \Omega_B\chi_B + E, \quad (8)$$

where Υ and E are the vectors of 'stacked' actual motor torques and model errors respectively, all of a size $[r \times 1]$ with $r = n \cdot n_e$ and n_e being the number of measurement samples; Ω_B is the *IDM observations matrix* vertically stacked from $\omega_B\left(q(t_k),\dot{q}(t_k),\ddot{q}(t_k)\right)$ blocks for $k = 1,\ldots,n_e$, Janot et al. (2014).

3. OPTIMAL EXCITATION TRAJECTORIES

Successful identification of robot's dynamics relies on availability of a family of rich-in-modes robot's nominal trajectories $q_i^*(\cdot)$. Performing them in experiments the robot will provide the input data for computing estimates of model parameters based on the linear regression (6). For various reasons (see e.g. Swevers et al. (1997)) it is convenient to consider a parametric family of nominal trajectories, where behaviors of joint coordinates are trigonometric polynomials of time, i.e. when the motion of i^{th}-joint ($i = 1,\ldots,n$) is written as

$$q_i^\star(t) = q_{i,0} + \sum_{k=1}^{n_f}\left[a_{i,k}\sin(kw_0t) + b_{i,k}\cos(kw_0t)\right]. \quad (9)$$

Here $q_{i,0}$ is the initial bias, w_0 is the base frequency, $a_{i,k}$ and $b_{i,k}$ are constant coefficients, n_f is the number of frequencies.

Searching coefficients $\{a_{i,k}, b_{i,k}\}$ of trigonometric polynomials (9) are commonly done through solving appropriately posted constrained optimization problem.

Remark 3. The order n_f of the polynomials and their base frequency w_0 are selected in advance. They should respond to requirements for inducing high-frequency modes ($w_0 \uparrow, n_f \uparrow$) and for covering a larger part of the robot workspace ($w_0 \downarrow$). However, they cannot be any and, in particular, to avoid an excitation of a hidden dynamics in

transmission, the parameters should be consistent with the inequality $n_f \cdot w_0 < w_r$, where w_r is the smallest resonance frequency among the joints.

Some of constraints for optimization can be taken directly from the list of robot specifications representing limits imposed on joints' variables and their velocities. Others, such as geometrical constraints representing conditions for obstacle avoidance, self-occlusion and imposed in the workspace of the robot, require volumetric characteristics of a robot structure combined with the forward kinematics.

Another important constraints, such as torques limits, require an iterative use of the model (1)-(4) with the current update of parameters available to the moment. Additional constraints can be enforced due to implementation conditions, e.g. zero joints' velocities and accelerations at the beginning and the end of a searched motion.

In order to achieve a coherent distribution of behaviors among joints, one can follow the common strategy and consider the optimization index defined as the condition number of the IDM observation matrix $\Omega_B(\cdot)$, i.e. $\texttt{cond}\,(\Omega_B) \to \min$. However, such choice might lead to trajectories with lack of sufficient excitation of weakly loaded wrist joints, bad signal-to-noise ratios of recorded data and potentially result in inaccurate estimates for their dynamic parameters.

We have tested the applicability of *multiobjective optimisation* as one of alternatives for exciting the dynamics of the last two joints. The formal settings of such optimisation assignment have been the following: [2]

$$\min_{\substack{q_{i,0}\\ a_{i,k},b_{i,k}}} \gamma \quad \texttt{s.t.} \begin{cases} F\left(q_{i,0}, a_{i,k}, b_{i,k}, t\right) - \gamma \cdot \Psi \le \Lambda, \\ [\dot{q}_i^\star(0),\, \ddot{q}_i^\star(0)] = [0,\, 0], \\ q_i^\star(t) \in (q_{i,min}, q_{i,max}), \\ \dot{q}_i^\star(t) \in (\dot{q}_{i,min}, \dot{q}_{i,max}), \\ \tau_i^\star(t) \in (\tau_{i,min}, \tau_{i,max}), \\ i = 1 \ldots n, \quad k = 1 \ldots n_f \\ d_{xy}(t) \ge 0.3,\ z(t) \ge -0.2. \end{cases} \tag{10}$$

Here $\Lambda = [g_{\Omega_b}; k_{\tau_6} \cdot \tau_{6,max}; k_{\tau_7} \cdot \tau_{7,max}]$ is the goal matrix, γ is the attainment coefficient, $\Psi = |\Lambda|$ is the weight matrix, and

$$F(\cdot) = \left[\texttt{cond}\,(\Omega_B)\,; \overline{(\tau_{6,max} - |\tau_6^\star(t)|)}; \overline{(\tau_{7,max} - |\tau_7^\star(t)|)}\right]$$

can be interpreted as the vector objective function, where $\overline{(\cdot)}$ denotes a mean value [3] of an argument over time-interval it is defined.

Remark 4. The goal matrix parameters g_{Ω_b}, k_{τ_6}, and k_{τ_7} can largely affect the optimisation results and should be carefully selected. A way to find its approximate values is to perform a single criterion optimisation (such as $\texttt{cond}\,(\Omega_B) \to \min$) in advance.

4. PARAMETER ESTIMATION

Initially, the problem of the dynamic model identification can be formulated as finding estimates $\hat{\chi}_B$ of the base IDM parameters that minimise discrepancies $\Delta\Upsilon$ between measured and calculated motor torques along stacked for the whole identification trajectory

$$||\Delta\Upsilon|| \to \min, \tag{11}$$

where $\Delta\Upsilon = \Upsilon_m - \Upsilon(\hat{\chi}_B) = \tau_m - \omega_B\left(q_m, \dot{q}_m, \ddot{q}_m\right)\hat{\chi}_B$.

Commonly, raw measurements of $\tau(\cdot)$ and $q(\cdot)$ are pre-processed by band-pass filtering for reducing noise and for estimating velocities and accelerations resulting into the *Inverse Dynamic Identification Model (IDIM)*

$$\Upsilon_f = \Omega_{Bf}\chi_B + E_f, \tag{12}$$

where the index f denotes filtered data

$$\Upsilon_f = \left[\tau^f(t_1); \tau^f(t_2); \ldots \tau^f(t_{n_e})\right],$$

$$\Omega_{Bf} = \begin{bmatrix} \omega_B\left(\hat{q}^f(t_1), \hat{\dot{q}}^f(t_1), \hat{\ddot{q}}^f(t_1)\right) \\ \vdots \\ \omega_B\left(\hat{q}^f(t_{n_e}), \hat{\dot{q}}^f(t_{n_e}), \hat{\ddot{q}}^f(t_{n_e})\right) \end{bmatrix}.$$

We assume here that the filtered error signal E_f in Eqn. (12) has zero mean, serially uncorrelated and heteroskedastic (see e.g. Janot et al. (2014)). It implies that E_f has a block-diagonal covariance matrix

$$R = \text{diag}\left(\sigma_1^2\mathbf{I}_{ne}, \cdots, \sigma_j^2\mathbf{I}_{ne}, \cdots, \sigma_n^2\mathbf{I}_{ne}\right), \tag{13}$$

where I_{ne} is the $[n_e \times n_e]$ identity matrix and σ_j^2 is the error variance calculated from j-th subsystem of Eqn. (12).

In these settings the optimal-in-variance estimates for elements of the vector χ_B are provided by the Weighted Least Squares (WLS) algorithm

$$\hat{\chi}_B = \left(\Omega_{Bf}^T R^{-1}\Omega_{Bf}\right)^{-1}\Omega_{Bf}^T R^{-1}\Upsilon_f. \tag{14}$$

The covariance matrix of such estimate given by

$$\Sigma = \left(\Omega_{Bf}^T R^{-1}\Omega_{Bf}\right)^{-1}$$

quantitatively describes the parametric uncertainty in $\hat{\chi}_B$ as a whole, while the *relative standard deviation* (RSD) of the i-th element in $\hat{\chi}_B$

$$\%\bar{\sigma}_{\hat{\chi}_B^i} = \frac{100 \cdot \bar{\sigma}_{\hat{\chi}_B^i}}{\left|\hat{\chi}_B^i\right|}, \tag{15}$$

can be used as a certificate for each individual characteristic, where $\bar{\sigma}^2_{\hat{\chi}_B^i}$ is the i-th diagonal coefficient of Σ.

In turn, some of the base IDM parameters might not have a significant contribution to the system dynamics and can be post-eliminated reducing a set of the base parameters to a smaller set of *essential IDM parameters*. Systematically it can be done using statistical hypothesis tests as described in **?**. However, if identification steps for both motor and joint dynamics are performed concurrently, then one needs to keep among essential parameters those, which can be only estimated in hard-to-excite modes. In this case, a manually supervised iterative elimination procedure can be implemented as an alternative see e.g. Briot et al. (2014)).

The approach allows an efficient software realization of the identification procedure, however the justification of the validity of the assumptions that support the method should be clearly performed in each case study. In general, they are met provided that measurements $q(\cdot)$ and $\tau(\cdot)$ are acquired at high sampling rate and the data filtering are well tuned.

[2] The problem is specified in a form adapted for implementation with the Matlab *'fgoalattain'* function.

[3] Values for limits of joint angles, velocities, and torques can be found in the KUKA LWR4+ data-sheet.

5. CASE STUDY ON KUKA LWR4+ MODEL IDENTIFICATION

All the generic arguments for modelling and identification discussed above were applied for reconstructing dynamic models of the KUKA LWR4+ robotic arm. For consistency of identification results, experiments were prepared and run on the original KUKA LWR4+ and on the robot equipped with additional payload firmly attached to the last joint. The payload was ≈ 3.28 $[kg]$ with an off-set of the center of mass away from the axis of rotation of joint 7 for better excitation, see Fig. 1. In modeling and identification processes it was treated as the link 8 fixed to the link 7 of the robot. The discussion and

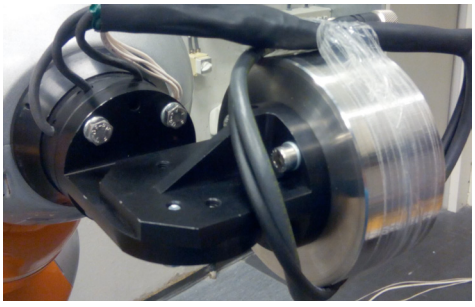

Fig. 1. Load for dynamics identification

data presented below are related to experiments with the payload attached. Similar to Jubien et al. (2014b), we considered three models for identification:

Model 1 captures primarily the robot dynamics neglecting the dynamics of motors, i.e. Eqn. (2) is replaced by the identity $\tau = \tau_l$. The approach is appropriate when measurements of joints' torques are only available and when motors' parameters are out of interest in application.

Model 2 captures both links and motors dynamics, i.e. the IDM is calculated for the complete set of Eqns. (1)–(4). The model assumes that motors and joints torques' measurements are both available.

Model 3 captures the motors' parameters appeared in Eqn. (2) and Eqn. (4). Identifying such model requires both motor and joint torque measurements, but, in contrast to Model 2, it relies on difference between these signals. Such approach allows estimating parameters of the motors dynamics gained independently of properties of the robot dynamics.

The *Symoro+* package (see Khalil and Creusot (1997)) was used both for symbolic representations of the corresponding regressions (6) and for the automatic selection of their base parameters. Consequently, a smaller subset of essential parameters was extracted for each model through a manually supervised iterative procedure (see Briot et al. (2014)). For example, for the most complete Model 2 written originally with $136 (= 8 \cdot 17)$ IDM parameters (for 7 joints and a payload) the *Symoro+* package found *eighteen* non-identifiable parameters and suggested other *sixteen* to be regrouped resulting altogether in the set of *base parameters* with 102 elements. *Forty nine* of them were later singled out by the manually supervised iterative procedure as *essential*. Regrouping relations for base parameters are similar to ones reported in (Jubien et al., 2014b, Table III). The developed symbolic representations were exported to Matlab and further used in planning of excitation trajectories and in computing estimates for parameters found essential.

Planning of excitation trajectories for the derived symbolic representations was approached and reformulated as optimization problems for searching coefficients of polynomials (9) in two different settings:

Trajectory A is calculated as a result of the single-objective optimization $\texttt{cond}\,(\Omega_B) \to \min$;

Trajectory B is calculated as a result of the multi-objective optimization (10) with $g_{\Omega_b} = 35$, $k_{\tau_6} = k_{\tau_7} = 0.9$.

Numerically, it was implemented using *Matlab Optimization Toolbox*. We performed planning for different base periods T_0 in (9) ranging between 10 and 30 sec, i.e. $w_0 = 1/T_0 = 0.05$ Hz and for number of harmonics $n_f = 5$. To illustrate advantages of the proposed trajectory planning procedure we compared major characteristics of three different excitation trajectories: trajectories A and B, and a non-optimized trajectory, when robot travels through 20 randomly selected configurations reaching maximum velocity and acceleration allowed by LWR's native motion planner. These characteristics include condition number of the IDM observation matrix, compliance with imposed kinematic and dynamic constraints, and an average joint torque magnitude as a metric for signal-to-noise ratio and are reported in Tab. 1.

Measured and filtered joint velocities and torques corresponding to excitation Trajectory B planned for Model 2 with $T_0 = 25$ sec are shown on Figs. 2a–2b.. As seen, the found trajectory is aggressive and covers most of the robot's workspace.

To command reference trajectories we activated the LWR4+'s *joint position control mode*. Reflexxes On-Line Motion Library available via Stanford FRI Library [4] was used to generate smooth trajectories from an arbitrary pose to a start pose of the excitation trajectory.

The dynamics identification experiment is demonstrated in the video (follow Kolyubin (2016) link).

The next step of the proposed dynamics identification routine is the acquired data processing to obtain parameters' estimates. To filter measured signals we set cut-off frequencies of $10Hz$ for 4^{th}-order band-pass Butterworth filters, and $2Hz$ for decimate filters. As we see, both cut-off frequencies are significantly higher than the maximum excitation frequency $n_f \cdot w_0 = 0.25$ Hz.

Some of the results of the base parameters identification are in Tab. 2. This table includes estimated values for 49 essential parameters and its RSDs $\%\bar{\sigma}_{\hat{\chi}_B^i}$ obtained for Model 2.

Finally, we performed computed torque tests to justify accuracy of the obtained parameters estimates. Several illustrative plots are presented in Fig. 3.

[4] `http://cs.stanford.edu/people/tkr/fri/html/index.html`

Table 1. Excitation trajectories characteristics

Trajectory	Constraints complied	Condition number	Mean torque $\overline{\lvert\tau_1\rvert}, \ldots \overline{\lvert\tau_7\rvert}$
Random points	yes	84.21	[3.05, 45.09, 6.78, 18.58, 2.17, 2.28, 1.04]
Optimized, Alg. 1	yes	34.01	[3.12, 41.71, 9.30, 13.24, 2.12, 1.56, 0.92]
Optimized, Alg. 2	yes	37.23	[4.63, 42.26, 10.23, 14.05, 1.56, 1.64, 1.64]

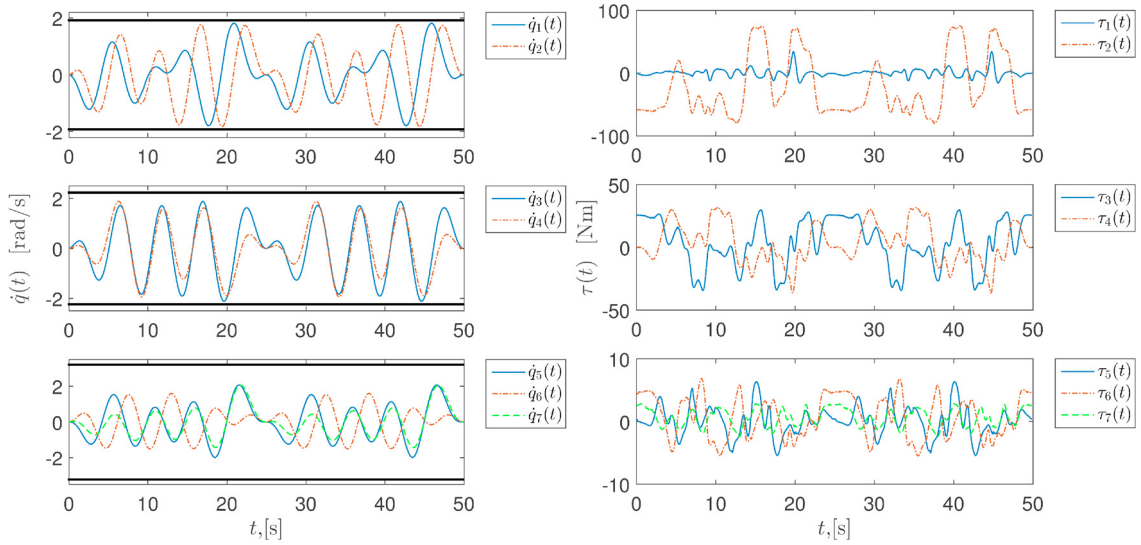

(a) Joint velocities (b) Joint torques

Fig. 2. An example of excitation trajectory

Table 2. Essential base parameters estimates for Model 2

Par.	$\hat{\chi}_B$	$\%\bar{\sigma}_{\hat{\chi}_B^i}$	Par.	$\hat{\chi}_B$	$\%\bar{\sigma}_{\hat{\chi}_B^i}$	Par.	$\hat{\chi}_B$	$\%\bar{\sigma}_{\hat{\chi}_B^i}$
$\mathbf{Ia_1}$	3.14	1.68	$\mathbf{Fvm_1}$	16.68	0.84	$\mathbf{Fcm_1}$	15.04	1.02
$\mathbf{Ia_2}$	2.58	5.42	$\mathbf{Fvm_2}$	19.09	1.29	$\mathbf{Fcm_2}$	16.48	1.43
$\mathbf{offm_2}$	2.09	6.91	$\mathbf{Ia_3}$	2.14	1.85	$\mathbf{Fvm_3}$	7.87	1.14
$\mathbf{Fcm_3}$	8.77	1.12	$\mathbf{Ia_4}$	1.97	4.20	$\mathbf{Fvm_4}$	11.63	1.61
$\mathbf{Fcm_4}$	9.96	2.11	$\mathbf{Ia_5}$	0.67	8.37	$\mathbf{Fvm_5}$	5.39	1.87
$\mathbf{Fcm_5}$	5.58	1.47	$\mathbf{Ia_6}$	0.38	6.51	$\mathbf{Fvm_6}$	3.64	1.63
$\mathbf{Fcm_6}$	4.41	1.41	$\mathbf{Ia_7}$	0.42	3.18	$\mathbf{Fvm_7}$	2.03	1.78
$\mathbf{Fcm_7}$	4.16	1.62	$\mathbf{offm_7}$	-0.54	7.31	$\mathbf{Fcl_1}$	0.79	2.70
$\mathbf{offl_1}$	0.28	7.33	$\mathbf{Fcl_2}$	0.41	2.24	$\mathbf{offl_2}$	-0.87	1.37
$\mathbf{Fcl_3}$	0.22	2.85	$\mathbf{Fcl_4}$	0.17	4.63	$\mathbf{offl_4}$	0.26	2.97
$\mathbf{Fcl_5}$	0.35	2.47	$\mathbf{offl_5}$	0.10	8.12	$\mathbf{Fcl_7}$	0.34	6.05
$\mathbf{offl_7}$	0.29	6.96	$\mathbf{XX_{2R}}$	1.36	0.93	$\mathbf{ZZ_{2R}}$	1.40	1.01
$\mathbf{MY_{2R}}$	3.46	0.06	$\mathbf{XX_{4R}}$	0.44	0.58	$\mathbf{ZZ_{4R}}$	0.45	0.73
$\mathbf{MY_{4R}}$	-1.37	0.08	$\mathbf{MY_{5R}}$	0.04	1.89	$\mathbf{MY_{6R}}$	0.03	3.23
$\mathbf{XX_8}$	0.09	2.65	$\mathbf{YY_8}$	0.07	3.85	$\mathbf{YZ_8}$	0.03	5.03
$\mathbf{ZZ_8}$	0.02	12.70	$\mathbf{MY_8}$	-0.22	0.55	$\mathbf{MZ_8}$	0.48	0.34
$\mathbf{M_8}$	3.34	0.09						

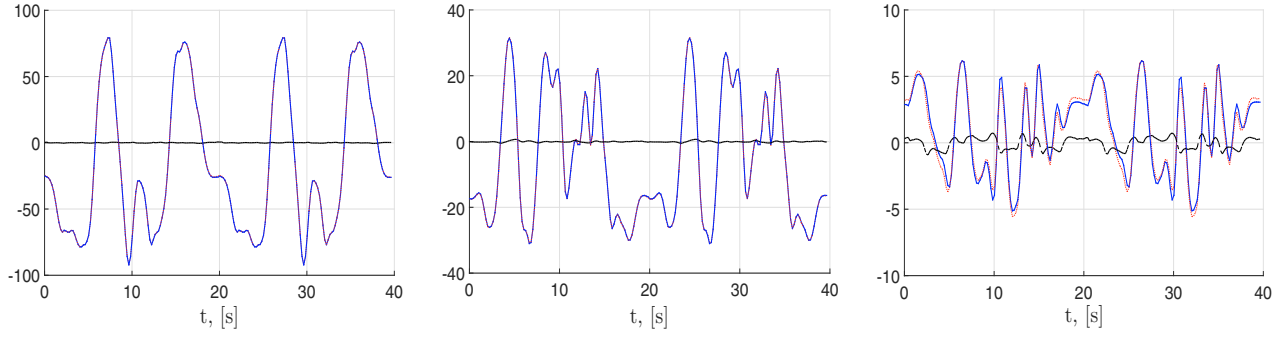

(a) Joint 2 (b) Joint 4 (c) Joint 6

Fig. 3. Computed-torque test for Model 2: measured(solid blue) and computed (dotted red) joint torques, and its relative error (dashed black)

6. CONCLUSIONS AND DISCUSSION

We reported experimental results of the KUKA LWR4+ serial redundant manipulator calibration. Our believe is that this is the most rigorous case-study in comparison with available before. Several conclusions come from this study.

Advancements in calibration trajectories optimisation allowed us to significantly increase tolerances of the obtained estimates. With the proposed multi-objective trajectories optimization approach we were able to shrink estimates' RSDs twice.

Robot-to-robot parameters variations can reach 20%. It emphasizes importance of the sequential kinematic and dynamic calibration and proves that CAD-based parameters values can serve as rough estimates only.

The biggest variations in parameters estimates are related to friction coefficients and drive parameters, which can be explained by the influence from the internal and external wiring, manufacturing tolerances, and wear-and-tear.

As further steps in this research direction, identification approaches providing better convergence under relaxed excitation conditions are required. In this sense, the approach described in Aranovskiy et al. (2016) can be a good alternative to the existing techniques.

REFERENCES

Aranovskiy, S., Bobtsov, A., Ortega, R., and Pyrkin, A. (2016). Parameters estimation via dynamic regressor extension and mixing. *Proc. of the American Control Conf.*, July, 6971–6976.

Bargsten, V., Zometa, P., and Findeisen, R. (2013). Modeling, parameter identification and model-based control of a lightweight robotic manipulator. In *2013 IEEE International Conference on Control Applications (CCA)*, 134–139. Institute of Electrical & Electronics Engineers (IEEE).

Briot, S., Gautier, M., and Jubien, A. (2014). In situ calibration of joint torque sensors of the kuka lightweight robot using only internal controller data. In *2014 IEEE/ASME International Conference on Advanced Intelligent Mechatronics*, 470–475.

Featherstone, R. and Orin, D.E. (2008). Dynamics. In B. Siciliano and O. Khatib (eds.), *Springer Handbook of Robotics*, 35–65. Springer Berlin Heidelberg.

Gautier, M. and Khalil, W. (1990). Direct calculation of minimum set of inertial parameters of serial robots. *IEEE Trans. Robot. Automat.*, 6(3), 368–373.

Gaz, C., Flacco, F., and Luca, A.D. (2014). Identifying the dynamic model used by the kuka lwr: A reverse engineering approach. In *2014 IEEE International Conference on Robotics and Automation (ICRA)*, 1386–1392. Institute of Electrical & Electronics Engineers (IEEE).

Hollerbach, J., Khalil, W., and Gautier, M. (2008). Model identification. In B. Siciliano and O. Khatib (eds.), *Springer Handbook of Robotics*, 321–344. Springer Berlin Heidelberg.

Janot, A., Vandanjon, P.O., and Gautier, M. (2014). A generic instrumental variable approach for industrial robot identification. *IEEE Transactions on Control Systems Technology*, 22(1), 132–145.

Jubien, A., Gautier, M., and Janot, A. (2014a). Dynamic identification of the kuka lightweight robot: Comparison between actual and confidential kuka's parameters. In *2014 IEEE/ASME International Conference on Advanced Intelligent Mechatronics*, 483–488. Institute of Electrical & Electronics Engineers (IEEE).

Jubien, A., Gautier, M., and Janot, A. (2014b). Dynamic identification of the Kuka LWR robot using motor torques and joint torque sensors data. *IFAC Proceedings Volumes (IFAC-PapersOnline)*, 19, 8391–8396.

Khalil, W. and Dombre, E. (2004). *Modeling, Identification and Control of Robots*. Elsevier Science.

Khalil, W. and Gautier, M. (1991). Calculation of the identifiable parameters for robot calibration. In *The 9th IFAC/IFORS Symposium on Identification and System Parameter Estimation*, 888–892. Budapest, Hungary.

Khalil, W., Gautier, M., and Enguehard, C. (1991). Identifiable parameters and optimum configurations for robots calibration. *Robotica*, 9(01), 63–70.

Khalil, W. and Creusot, D. (1997). SYMORO+: a system for the symbolic modelling of robots. *Robotica*, 15(2), 153–161.

Kolyubin, S. (2016). LWR dynamics calibration experimental demo. YouTube Video. URL https://youtu.be/dCzI3Pgs1P0.

Rackl, W., Lampariello, R., and Hirzinger, G. (2012). Robot excitation trajectories for dynamic parameter estimation using optimized b-splines. In *Robotics and Automation (ICRA), 2012 IEEE International Conference on*, 2042–2047.

Swevers, J., Ganseman, C., Tukel, D., de Schutter, J., and Brussel, H.V. (1997). Optimal robot excitation and identification. *IEEE Trans. Robot. Automat.*, 13(5), 730–740.